

KAUNAS UNIVERSITY OF TECHNOLOGY

MARIUS ANDRIKAITIS

**MODELING AND RESEARCH OF CRITICAL
REGIMES OF THE SAILPLANE LAK-17B
STRUCTURE**

Summary of Doctoral Dissertation
Technological Sciences, Transport Engineering (03T)

2014, Kaunas

The dissertation was prepared in 2009 – 2013 at Kaunas University of Technology, Institute of Defense Technology.

Scientific supervisor:

Prof. Dr. Habil. Algimantas FEDARAVIČIUS, (Kaunas University of Technology, Technological Sciences, Transport Engineering – 03T).

Dissertation Defense Board:

Prof. Dr. Habil. Vytautas OSTAŠEVIČIUS (Kaunas University of Technology, Technological Sciences, Transport Engineering – 03T) – chairman,
Prof. Dr. Žilvinas BAZARAS (Kaunas University of Technology, Technological Sciences, Transport Engineering – 03T),
Prof. Dr. Habil. Marijonas BOGDEVIČIUS (Vilnius Gediminas Technical University, Technological Sciences, Transport Engineering – 03T),
Prof. Dr. Artūras KERŠYS (Kaunas University of Technology, Technological Sciences, Transport Engineering – 03T),
Prof. Dr. Romualdas KLIUKAS (Vilnius Gediminas Technical University, Technological Sciences, Mechanical Engineering – 09T).

Official Opponents:

Dr. Rolanas DAUKŠEVIČIUS (Kaunas University of Technology, Technological Sciences, Mechanical Engineering – 09T),
Prof. Dr. Habil. Jonas STANKŪNAS (Vilnius Gediminas Technical University, Technological Sciences, Transport Engineering – 03T).

The official defense of the dissertation will be held at 3 p.m. on 17th of December, 2014 at the Board of Transport Engineering Science Field public meeting in the Dissertation Defense Hall at the Central Building of Kaunas university of Technology.

Address: K.Donelaičio St. 73 – 403, LT-44029, Kaunas, Lithuania,
Phone nr. (+370) 37 300042, Fax. (+370) 37 324144,
e-mail: doktorantura@ktu.lt

The summary of dissertation was sent on 17th of November, 2014.

The dissertation is available at the library of Kaunas University of Technology (K.Donelaičio St. 20, LT-44239, Kaunas, Lithuania).

KAUNO TECHNOLOGIJOS UNIVERSITETAS

MARIUS ANDRIKAITIS

**SKLANDYTUVO LAK-17B KONSTRUKCIJOS
KRITINIŲ REŽIMŲ MODELIAVIMAS IR
TYRIMAS**

Daktaro disertacijos santrauka
Technologijos mokslai, transporto inžinerija (03T)

2014, Kaunas

Disertacija rengta 2009 – 2013 metais Kauno Technologijos universitete, Gynybos technologijų institute.

Mokslinis vadovas:

Prof. habil. dr. Algimantas FEDARAVIČIUS, (Kauno technologijos universitetas, technologijos mokslai, transporto inžinerija – 03T).

Disertacijos gynimo taryba:

Prof. habil. dr. Vytautas OSTAŠEVIČIUS (Kauno technologijos universitetas, technologijos mokslai, transporto inžinerija – 03T) – pirmininkas,

Prof. dr. Žilvinas BAZARAS (Kauno technologijos universitetas, technologijos mokslai, transporto inžinerija – 03T),

Prof. habil. dr. Marijonas BOGDEVIČIUS (Vilniaus Gedimino technikos universitetas, technologijos mokslai, transporto inžinerija – 03T),

Prof. dr. Artūras KERŠYS (Kauno technologijos universitetas, technologijos mokslai, transporto inžinerija – 03T),

Prof. dr. Romualdas KLIUKAS (Vilniaus Gedimino technikos universitetas, technologijos mokslai, mechanikos inžinerija – 09T).

Oficialieji oponentai:

Dr. Rolanas DAUKŠEVIČIUS (Kauno technologijos universitetas, technologijos mokslai, mechanikos inžinerija – 09T),

Prof. habil. dr. Jonas STANKŪNAS (Vilniaus Gedimino technikos universitetas, technologijos mokslai, transporto inžinerija – 03T).

Disertacija bus ginama viešame transporto inžinerijos mokslo krypties tarybos posėdyje, kuris įvyks 2014 m. gruodžio 17 d. 15 val., Kauno technologijos universitete, Centrinų rūmų disertacijų gynimo salėje.

Adresas: K.Donelaičio g. 73 – 403, LT-44029, Kaunas, Lietuva,
Tel. (8 - 37) 300042, faksas (8 - 37) 321444, e. paštas: doktorantura@ktu.lt

Daktaro disertacijos santrauka išsiųsta 2014 lapkričio 17 d.

Disertaciją galima peržiūrėti Kauno technologijos universiteto bibliotekoje (K.Donelaičio g. 20, LT-44239, Kaunas, Lietuva).

INTRODUCTION

General

In order to get type certificate for a newly designed aircraft, the compliance with corresponding certification requirements must be shown.

During the certification process, the compliance with the requirements is demonstrated by performing flight and ground tests. With the development of computer hardware and computational methods, the number of cases, when requirements are met based on the use of numerical methods, is increasing.

This work can be divided into two main parts: (a) development of numerical models and (b) analysis of the sailplane critical regimes using these models. The goal of the analysis is to determine whether the structure complies with certification requirements.

The term "critical regimes" herein are used to define the limit static and dynamic load cases of the sailplane. Considered regimes: (a) main landing gear ground load conditions, (b) fuselage and tail surfaces flight load conditions, (c) empennage flutter.

The object being modeled and analyzed is Lithuanian aviation construction – 15/18-meter class sailplane LAK-17B.

LAK-17B is a modification of a certified sailplane LAK-17A. The main difference between these sailplanes is wing design. Other systems of the LAK-17B sailplane – fuselage, tail surfaces, landing gear – are the same as in LAK-17A.

During the certification process of the LAK-17A, the manufacturer of the sailplane performed the flight and ground testing to show the compliance with certification requirements.

In general, there are three methods to show the compliance with certification requirements: (a) testing, (b) numerical modeling (c) testing and numerical modeling. Authorities that create the certification requirements define conditions of use of each method. This work is based on the certification specifications for sailplanes and powered sailplanes CS-22 [1] developed by European Aviation Safety Agency (EASA).

To show the compliance with strength and deformation requirements, CS-22 allows the use of structural analysis if the structure conforms to those for which experience has shown this method to be reliable. In other cases, substantiating load tests must be made.

To show that the sailplane is free from flutter, CS-22 requires: (a) to perform ground vibration test which includes an analysis and an evaluation of the established vibration modes and frequencies for the purpose of recognizing combinations critical for flutter, either by an analytical method, or any other approved method; (b) to perform systematic flight tests to induce flutter.

Research methods

This work was made using methods of theoretical research (numerical modeling). To evaluate numerical models reliability, test data were used. All the test data were supplied by the sailplane manufacturer.

The finite element models were made using MSC.Patran software. Strength, buckling and flutter analyses were performed using MSC.Nastran software with MSC.FlightLoads module. The auxiliary models were implemented using spreadsheet software.

Dissertation structure

Dissertation has 111 pages, 102 numbered equations, 115 figures and 24 tables.

Dissertation consists of introduction, five chapters, general conclusions and bibliography.

The first chapter focuses on: (a) competition classes in gliding and common characteristics of the sailplanes of the same class, (b) ground and flight loads evaluation according to certification specifications CS-22, (c) numerical modeling and research methods of the aircraft structures according to scientific and technical publications.

The second chapter describes algorithm used to study the critical regimes of the sailplane and analyzes the underlying theory. The following methods that are implemented in selected FEA software were studied: (a) modeling of laminar composites and composite failure theories, (b) normal modes evaluation and flutter analysis.

The third chapter describes modeling techniques used to create sailplane numerical models. The main components of the sailplane – fuselage, wings, tail surfaces and landing gear – are studied.

The fourth chapter describes the evaluation procedure of the model parameters. In this work, the model parameter set consist of a set of applied loads, a set of points coordinates that represent the locations of applied loads and the values that represent optimal finite element mesh density.

The fifth chapter provides the sailplane's critical regimes analysis results. The following data were obtained using numerical modeling: (a) ultimate loads acting on the main landing gear and the factor of safety of the main landing gear leg, (b) factors of safety of the fuselage and tail surfaces, (c) critical flutter speeds of the sailplane.

Aim of the Research

The aim of this research is to develop numerical models of the LAK-17B sailplane and investigate its critical regimes in order to prove that the structure complies with the certification requirements.

Objectives of the Research

1. Create numerical models of the main components of the LAK-17B sailplane (landing gear, fuselage and aerodynamic surfaces) and demonstrate that these models are reliable for analyzing selected critical regimes of the sailplane.
2. Investigate the critical regimes of the main landing gear using created models.
3. Investigate the critical regimes of the fuselage and tail surfaces using created models.
4. Perform empennage flutter analysis using created models.

Scientific novelty

1. The created numerical models were used to investigate the impact of individual components' parameters variation on the overall system (the sailplane LAK-17B and its modifications).
2. It was discovered that the structure complies with the certification requirements.

Practical value

1. During this work, the sailplane's LAK-17B (and its modifications) numerical models creation methodology was developed.
2. The methodology was applied to create numerical models of the sailplane components.
3. The numerical models were used to investigate critical regimes of the LAK-17B sailplane.
4. The research results were implemented in the certification process of the sailplane LAK-17B.

Defended statements

1. The models used in analyses consider the following peculiarities of the LAK-17B sailplane: (a) geometrical characteristics, (b) hinge joints between different parts of the sailplane, (c) material characteristics of each layer of composite materials, (d) mass distribution.
2. The strength and stiffness of the landing gear of the LAK-17B sailplane comply with certification specifications for sailplanes and powered sailplanes CS-22.
3. The strength of the LAK-17B fuselage and tail surfaces does meet strength and deformation requirements of CS-22. In emergency landing case, the cockpit zone of the fuselage should be reinforced.
4. The sailplane oscillations inside the flight speeds range 90...150 km/h are caused by rudder flapping. Without modifying the rudder control system design, it is necessary and sufficient condition for eliminating these oscillations – fixing the rudder (keeping feet on the rudder pedals).

Approbation of the results

The results of this work are published in two articles in two reviewed periodic scientific journals.

The results of this work are presented in two international conferences.

The experience gained during this work was used during analysis of rotary wing aircraft. The results of research were presented in two international conferences.

1. LITERATURE REVIEW

This chapter considers the following problems: (a) competition classes in gliding and common characteristics of the sailplanes in the same class, (b) loads evaluation according to CS-22, (c) numerical modeling and research methods of aircraft structures according to scientific and technical publications.

2. METHODS USED IN RESEARCH

2.1. Research algorithm

Analysis of the sailplane was performed in two steps:

1. Development of numerical models.
2. Strength, buckling, and aeroelastic analyses using numerical models.

Model development procedure is described in third chapter of this work. Strength, buckling and flutter analysis was performed in steps:

1. Fuselage, tail surfaces and main landing gear strength analysis.
2. Fuselage and tail surfaces buckling analysis.
3. Sailplane modal analysis.
4. Flutter analysis of the sailplane.

Sailplane strength analysis was performed according to scheme shown at Fig. 2.1. Each component of the sailplane was analyzed two times. The first calculation stage was used to evaluate the quality of model. During the second stage of calculation the model was used to analyze the critical regimes of the structure. Two different parameter sets conforming to two different modifications of the sailplane were used in each stage. In this work, the model parameter set consist of (a) a set of applied loads, (b) a set of points coordinates that represent the locations of applied loads and (c) the values that represent optimal finite element mesh density. Calculation of model parameters is carried out at fourth chapter of this work.

The static tests results were used to evaluate the quality of finite element models. The tests data were compared to corresponding finite element analysis data. The accuracy of the model was considered acceptable if the discrepancy between the test data and FEA data is less than 10%. If the discrepancy between the test data and FEA data is greater than 10%, the finite element model is modified.

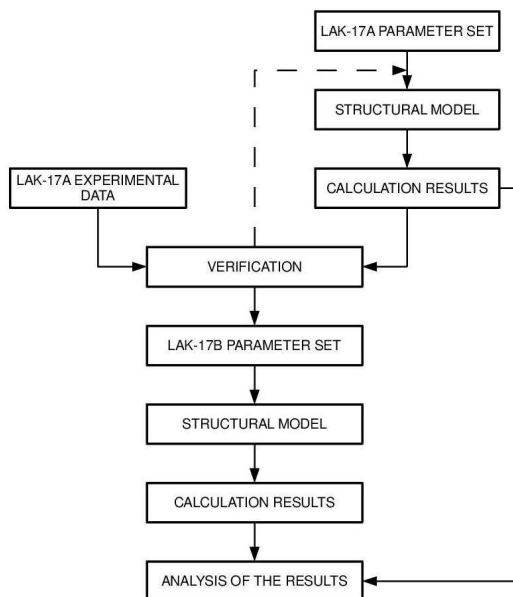


Fig. 2.1. Fuselage and tail surfaces strength analysis scheme

The strength of composites was evaluated using *maximum stress failure theory* – the *failure index*, representing the ratio between maximum stress and ultimate stress of the ply was studied for each layer of the composite material.

The fuselage and tail surfaces buckling analyses were performed according to scheme used for strength analysis (see Fig. 2.1). Each component of the sailplane was analyzed two times. The first calculation stage was used to evaluate the quality of model. During the second stage of calculation the model was used to analyze the critical regimes of the structure.

The tests data were used to evaluate the quality of the models. The same set of loads that made the construction to buckle during test was used to perform FEA. The tests data were compared to corresponding finite element analysis data. The accuracy of the model was considered acceptable if the *buckling load factor* calculated using finite element analysis is in range of $[0.9 \div 1.1]$. If the calculated buckling load factor is outside the range, the finite element model is modified.

The sailplane flutter analysis was performed in two steps:

1. Calculation of vibration modes.
2. Evaluation of diagrams of damping and frequency versus flight speed.

The vibration modes of the airframe were calculated for two sailplane configurations:

1. Sailplane of wingspan of 15 meters.

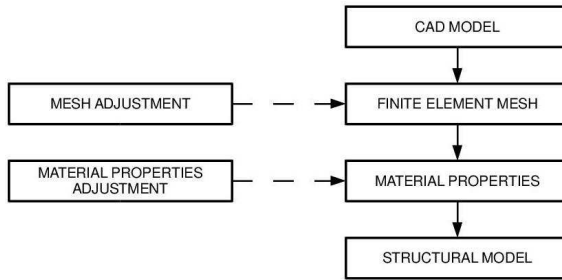


Fig 2.3. Numerical models development scheme

After modification of models according to scheme shown at Fig 2.3, the strength (see Fig. 2.1) and flutter (see Fig. 2.2) analyses are performed again.

3. DEVELOPMENT OF THE SAILPLANE NUMERICAL MODELS

3.1. The object being modeled

The numerical models of the sailplane LAK-17B were developed at this work. LAK-17B is a 15/18 meter class single-seat sailplane designed according to the certification specifications for sailplanes and powered sailplanes CS-22 [1].

The sailplane has T-tail and its wings consist of two parts. The outer parts of wings are interchangeable; therefore, the sailplane can be in 15 meter or 18 meter configuration.

LAK-17B is a modification of the certified sailplane LAK-17A. The major difference between these sailplanes is the construction of wings.

The wing of LAK-17B (see Fig. 3.1) consists of four parts: left and right inner wings *1*, left and right outer wings. There are two sizes of outer wings: 3500 mm length outer wings *3* are used for 18-meter configuration sailplane and 2000 mm length outer wings *2* are used for 15-meter configuration sailplane.

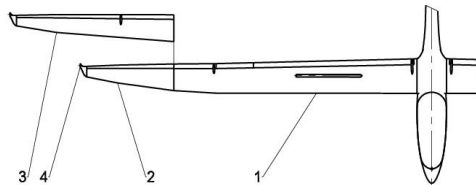


Fig. 3.1. Wing of the LAK-17B sailplane: *1* – inner wing; *2* – 2000 mm length outer wing; *3* – 3500 mm length outer wing; *4* – winglet

The wing of LAK-17A (see Fig. 3.2) consists of left and right wings *1* and left and right wingtips. There are two sizes of wingtips: 1650 mm length wingtips *2* are used for 18-meter configuration sailplane and 150 mm length wingtips *3* are used for 15-meter configuration sailplane.

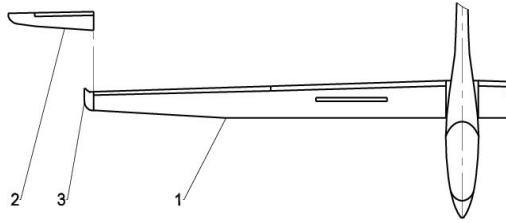


Fig. 3.2. Wing of the LAK-17A sailplane: 1 – wing; 2 – 1650 mm length wingtip; 3 – 150 mm length wingtip

Construction of wings is of one spar monocoque type. Their spars are 2-T shape in section. Carbon rods GRAPHLITE SM 315 are used for spar shelves. Wing shells are stuck of two parts: an upper and lower shell parts. The shell is of three-layer construction. External and internal shell layers are made of carbon and glass fiber. The outer layers are separated by foam. Thickness of foam of wing shells is 6 mm.

3.2. Development of numerical models

3.2.1. Airframe models

The finite element models of airframe parts were created using Quad4 and Tria3 shell elements of MSC.Nastran. The following procedures were used to generate finite element mesh (Fig. 3.3):

1. surfaces generation;
2. mesh seeding;
3. meshing;
4. equivalencing.

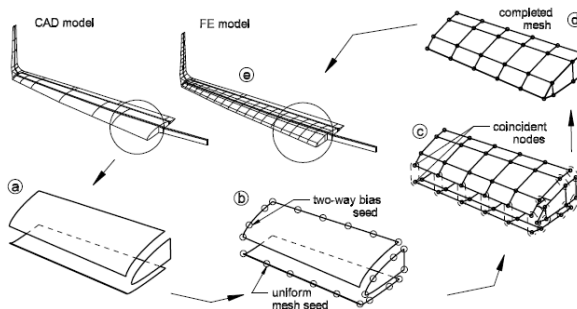


Fig. 3.3. The airframe modeling stages (shown on 15 m outer wing): a) surfaces generation; b) mesh seeding; c) meshing; d) equivalencing; e) finished mesh.

During first modeling stage, the complete sailplane was modeled as a collection of bi-parametric topologically congruent surfaces. That is, all the

adjacent surfaces shared a common edge. Surfaces were generated using 3D CAD modeling software.

Two types of mesh seeds were used to control model's mesh transition. Two-way bias seeds were used in chord-wise direction of aerodynamic surfaces to concentrate the element nodes near the leading edges and spars. The uniform mesh seeds were used in span-wise direction of aerodynamic surfaces and for the whole fuselage as well.

Automatic mesh generation tools of FEM pre-processor were used to mesh each individual surfaces of geometric model.

At equivalencing process, all the nodes that coexisted at a point were reduced to a single node. Equivalencing tolerance of 0.5 mm was used. The meshes that represent different parts were prevented from automatic nodes equivalencing by using minimal distance of 2 mm between these parts nodes.

After creating the meshes and applying composite material properties, finite element model stiffness was verified using experimental data.

3.2.2. Connections of parts

The meshes that represent different parts of the sailplane were connected to each other using multipoint constraints (MPCs) and beam elements.

Fig. 3.4 shows an example of how the hinges connecting rudder to the vertical tail plane were modeled.

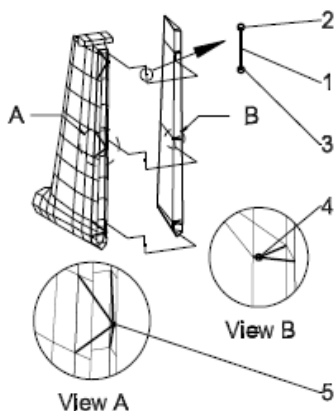


Fig. 3.4. Modeling of control surfaces hinges: 1 – beam element; 2, 3 – nodes of the beam element; 4, 5 – multipoint constraints.

The hinge is represented as a one-dimensional beam element (p. 1) with two nodes (p. 2, p. 3). Rotational behavior of the hinge is modeled by removing these nodes' rotational degrees of freedom around beam element's longitudinal axis from stiffness calculations.

Beam element's nodes are connected to rudder and fin meshes using MPCs (p. 4, p. 5).

Control system linkages were modeled using beam elements.

3.2.3. Control surfaces balance

The static moment of a real control surface is checked by measuring a component P of weight and the distance r between rotation axis and weighing point (Fig. 3.5 (a)). Then, a static moment of a control is calculated as follows:

$$M = P \cdot r \quad (3.1)$$

where: M - static moment; P - component of weight at a weighing point; r - static moment arm.

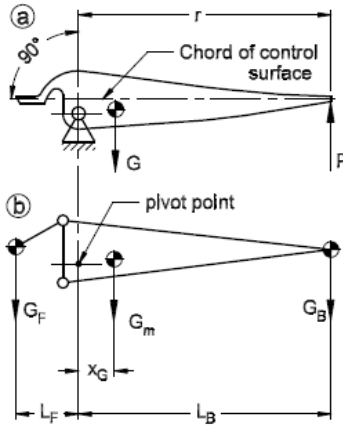


Fig. 3.5. Modeling of control surfaces: a) real control surface; b) FE model;

The FE models of control surfaces were modified by adding lumped masses at the front and the back of the surface (Fig. 3.5 (b)). Thus, the modeled and real control surfaces had the same static moments.

Front weight correction was calculated using equation:

$$G_F = \frac{G_m \cdot x_G + L_B(G - G_m) - r \cdot P}{L_F + L_B} \quad (3.2)$$

where: G – control surface weight; r – static moment arm; P – reaction force; G_F – front weight correction; G_m – FE model weight; L_F , x_G , L_B - distances between pivot point and concentrated weights.

After calculation of front weight correction, back weight correction is found as follows:

$$G_B = G - G_m - G_F \quad (3.3)$$

where: G – control surface weight; G_m – FE model weight; G_F – front weight correction; G – control surface weight.

Airframe mass distribution. After creating the meshes of the airframe parts and applying material properties, the initial mass of the model was m_M . That mass was modified to reflect the mass of an actual sailplane m_S by adding corrective masses m_C to the model.

Fig. 3.6 represents the mass correction procedure used for the fuselage model. The same procedure was applied to all the modeled parts of the airframe.

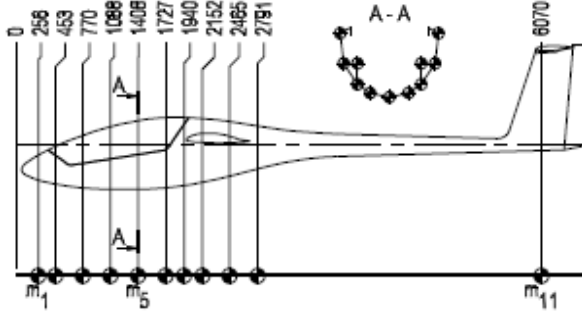


Fig. 3.6. Fuselage mass correction

Theoretical mass distribution was known – the fuselage was determined as a beam with attached masses m_i . These masses were reduced by subtracting fuselage model mass m_M :

$$m_c = \sum_{i=1}^n m_{c_i} = \sum_{i=1}^n \left(m_i - \frac{m_i \cdot m_M}{m_{fuselage}} \right) \quad (3.4)$$

where: m_C – corrective mass; m_i – fuselage segment mass; m_M – model mass; $m_{fuselage}$ – fuselage mass; n – number of corrective masses.

The calculated corrective masses m_{C_i} were distributed at corresponding sections of the fuselage finite element model as shown at Fig. 3.6.

3.2.4. Aerodynamic models

Lifting surfaces of the sailplane were modeled as a collection of flat panels (Fig. 3.7). Each panel was divided into elements. The following guidelines were observed in subdivision:

1. The dimensions of elements should be decreased in the directions and regions of large gradients in pressure and/or downwash.
2. The aspect ratio of each element should be less than or equal to 1.

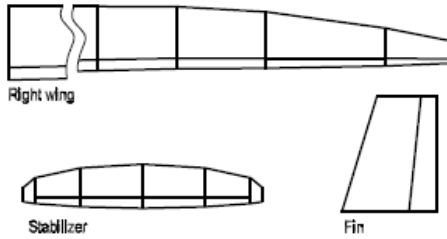


Fig. 3.7. Aerodynamic models of sailplane lifting surfaces (subdivision into elements not shown)

Other researchers have found that inclusion of slender bodies and interference elements in aerodynamic models increases calculated flutter velocity marginally [3]. Therefore, the fuselage of the sailplane was not modeled.

4. EVALUATION OF MODEL PARAMETER SETS

To be able to compare results of two numerical calculations, the same loads evaluation procedure was used for both finite element models. The loads were calculated for minimal and maximal sailplane weight, for all flaps positions and all flight conditions of the $v-n$ diagram. A chart of velocity versus load factor, or $v-n$ diagram shows the limits of aircraft performance. It shows how much load factor can be safely achieved at different airspeeds. The maneuvering speed V_A of an aircraft is an airspeed limitation selected by the designer or the aircraft. At speeds close to, and faster than, the maneuvering speed, full deflection of any flight control surface should not be attempted because of the risk of damage to the aircraft structure.

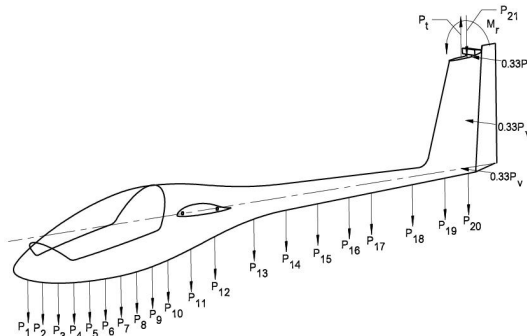


Fig. 4.1. Finite element model loads distribution scheme

The evaluated loads were applied to the sailplane finite element model according to distribution scheme shown at Fig. 4.1.

The parameters of the landing gear models were considered in this chapter as well.

Experimental data was used to verify the modeling results. The manufacturer of the sailplane supplied two types of static test results: displacements of the horizontal stabilizer specific points and strains at specific points of the fuselage shell structure.

5. INVESTIGATION OF CRITICAL REGIMES OF THE LAK-17B SAILPLANE

5.1. Main landing gear strength and deformation analysis

The results of main landing gear strength analysis are summarized in Table 5.1.

Table 5.1. Summary of main landing gear strength and deformation analyses results

Parameter	Calculated values	Valid values
Stress of main stand (LAK-17A) σ , MPa	148	$\sigma \leq 834$
Stress of main stand (LAK-17B) σ , MPa	150	$\sigma \leq 834$
Deflection of the tire d_r , mm	52	$d_r < 75$
Deflection of frame Δy^* , mm	17	$\Delta y^* < 23$
Ground reaction load factor n	4	$n \leq 4,5$

According to data of Table 5.1:

1. The stress of the most loaded part of the LAK-17B landing gear leg is 10% greater than the stress of the most loaded part of the LAK-17A landing gear leg, but more than 50% less than ultimate stress of the material.
2. Deflection of the tire is 70% of the permissible deflection. Deformation of the tire is not ultimate.
3. Deflection of the main landing gear leg (without the tire) is 75% of the permissible deflection. Deformation the main landing gear leg is not ultimate.
4. The ground reaction load factor is 4g. The ground reaction load factor does not exceed the permissible 4.5g limit [1].

5.2. Fuselage and tail surfaces strength analysis

The results of the fuselage and tail surfaces strength and buckling analyses are summarized in Table 5.2

Table 5.2. Summary of the fuselage and tail surfaces strength and buckling analyses results

Parameter	Calculated values		Valid values
	First step of analysis	Second step of analysis	
Combined loading case			
The layers of the rear part of fuselage that have max. failure indices (LAK-17A)	14, 15, 16	–	–
The layers of the rear part of fuselage that have max. failure indices (LAK-17B)	14, 15, 16	–	–

Parameter	Calculated values		Valid values
	First step of analysis	Second step of analysis	
The max. value of failure index FI	0.6	–	$FI \leq 1$
Buckling load factor k_F	1.2	–	$k_F \geq 1$
Emergency landing case			
The max. value of failure index FI	1.1	0.87	$FI \leq 1$
Buckling load factor k_F	0.96	1.2	$k_F \geq 1$
Horizontal tail strength analysis			
The max. value of failure index FI	0.64	–	$FI \leq 1$

In emergency landing case, the maximum failure index of the layers at the cockpit zone is greater than 1, and the buckling load factor is less than 1. According to these results, the cockpit zone should be reinforced.

The layout of the fuselage frontal part was modified. Additional three layers of glass cloth 92125 were included (ply angle – 0° according to longitudinal sailplane axis).

After finite element model modification, the emergency landing regime was analyzed second time. According to analysis results, the evaluated strength of cockpit zone is sufficient ($FI < 1$, and $k_F > 1$).

According to data of Table 5.2:

1. In the combined loading case, the most loaded layers of the fuselage shell are the 14th, 15th and 16th. The maximum failure index of these layers $FI_{max} = 0.6 < 1$, and the buckling load factor $k_F = 1.2 > 1$. According to these results, the fuselage of LAK-17B does meet the strength requirements of CS-22.
2. In emergency landing case, the maximum failure index of the layers at the cockpit zone $FI_{max} = 1.1 > 1$, and the buckling load factor $k_F = 0.96 < 1$. Therefore, the cockpit zone should be reinforced.
3. The maximum failure index of the layers of horizontal tail $FI_{max} = 0.64 < 1$. According to computation results, the horizontal tail of LAK-17B does meet the strength requirements of CS-22.

5.3. Empennage flutter analysis

During the ground vibration testing, it was found that the fuselage twisting mode and the first asymmetric wing bending mode have close natural frequencies [2], similar to the earlier version – LAK-17A. The flutter behavior of these modes is further investigated herein.

5.3.1. Normal modes calculation

The normal modes calculations were carried out for two sailplane configurations: 1) wing span of 15 meters; 2) wing span of 18 meters.

The results are shown at Table 5.3. Calculated frequencies are compared to corresponding frequencies measured during ground vibration tests (GVT).

Currently, only the 18m sailplane test results are available. The comparison between measured and computed frequencies confirmed the adequacy of mass and stiffness models, however, it should be noted that the numerically obtained frequencies of symmetric modes correspond to experimentally measured frequencies better than asymmetric wing and fuselage frequencies. The following reasons of results inconsistency were considered:

1. Inadequate fuselage moments of inertia due to simplified mass correction procedure described at this paper (non-structural masses, as pilot and equipment were distributed on airframe shell structure).
2. Different simulation and test conditions. During simulation, the model was unsupported. During GVT, the sailplane was supported at its CG by springs.

Table 5.3. Sailplane LAK-17B normal modes. Theoretical and experimental data.

No.	Oscillation form	Frequency, (Hz)		
		18 m		15 m
		FEA	GVT	FEA
1	Wing 1st symmetric bending	1.79	1.52	2.57
2	Wing 2nd symmetric bending	6.18	6.07	10.44
3	Wing 3rd symmetric bending	14.77	14.65	18.36
4	Wing 4th symmetric bending	25.35	22.86	–
5	Wing 1st asymmetric bending	4.59	4.15	7.09
6	Wing 2nd asymmetric bending	10.86	14.58	13.81
7	Wing 3rd asymmetric bending	22.41	22.3	28.20
8	Wing torsion	18.73	20.01	21.86
9	Fuselage bending in horizontal plane	8.49	10.98	8.68
10	Fuselage bending in vertical plane	9.25	11.23	9.03
11	Rudder flapping	0.05	–	0.05
12	Fuselage torsion	3.94	4.12	4.26

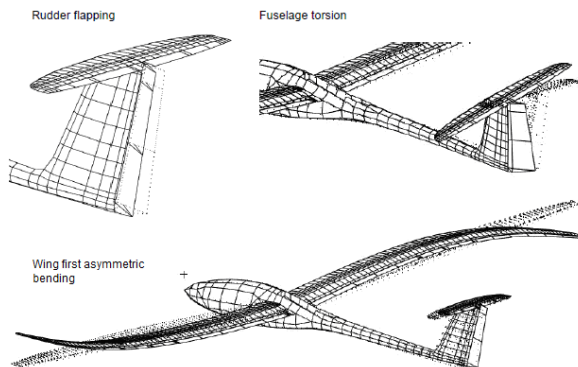


Fig. 5.1. Sailplane LAK-17B normal modes of interest

Two calculated modes of 18m wing span configuration had similar resonant frequencies: wing 2nd asymmetric bending (4.59 Hz) and fuselage torsion (3.94

Hz). Rudder flapping frequency depends on velocity; therefore, at certain flight speeds it might match the wing or fuselage frequencies as well.

These modes (Fig. 5.1) were selected for further empennage flutter analysis.

5.3.2. Flutter analysis

The analyses were performed for two configurations, corresponding to two wingspans of the sailplane: 1) wing span of 15 meters; 2) wing span of 18 meters. For each configuration, two conditions were simulated: 1) rudder fixed; 2) rudder free.

In all cases, the inherent damping of sailplane structure was neglected.

The flutter analysis was carried out for all the mode shapes of the sailplane up to frequency of 30 Hz in velocity range of (50 - 450) km/h.

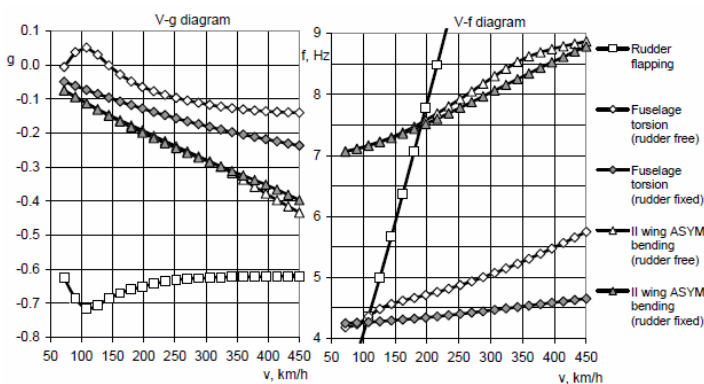


Fig. 5.2. V-g and V-f diagrams of sailplane LAK-17B with 15m wing span.

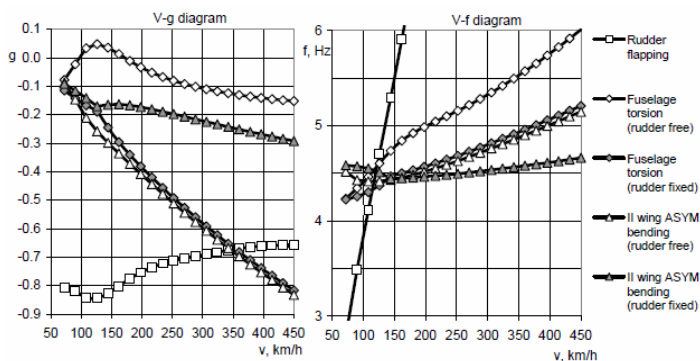


Fig. 5.3. V-g and V-f diagrams of sailplane LAK-17B with 18m wing span.

Fig. 5.2 shows the damping and frequency plots for rudder flapping, wing 2nd asymmetric bending and fuselage torsion of the sailplane with 15-meter wing span. The results of 18-meter configuration are shown at Fig. 5.3.

When rudder is free, fuselage torsion modes crosses the zero damping line in the v - g diagrams at 80km/h and crosses back over at 150km/h.

When the rudder is fixed, all the modes are below zero damping line in the v - g diagrams.

According to v - f diagrams, reduction of damping is caused by rudder flapping and fuselage torsion modes. The curves of these modes crosses at speed range of 90...120 km/h.

6. CONCLUSIONS

1. The created numerical models of the sailplane consider (a) geometrical characteristics, (b) hinge joints between different parts, (c) material characteristics of each layer of composite materials, (d) mass distribution. According to modeling and experimental data, (a) difference between theoretical and experimental deflections does not exceed 10%, (b) the location of buckling zone and buckling load factors evaluated using models correspond to experimental data, (c) the measured and calculated frequencies change in the same nature and the calculated mode shapes are the same as the ones obtained during test. The models are reliable for analyzing selected critical regimes of the sailplane.
2. The sailplane's LAK-17B main landing gear strength safety factor is greater than 1.5; the deflections of landing gear deformable parts are not ultimate, and the ground reaction load factor is 4g, which is less than maximum allowable value of 4.5g. The strength and stiffness of the landing gear of the LAK-17B sailplane comply with the certification specifications CS-22.
3. The factors of safety of the LAK-17B fuselage and tail surfaces are greater than 1.5, and the buckling load factor of the fuselage equals to 1.5. The strength of the fuselage and tail surfaces does meet strength and deformation requirements of CS-22. In emergency landing case, the factor of safety of the fuselage is less than 1.5; therefore, the cockpit zone of the fuselage should be reinforced.
4. According to evaluated v - g and v - f diagrams, the sailplane oscillations in the flight speeds range 90...150 km/h are caused by unbalanced rudder flapping. Without modifying the rudder control system design, it is necessary and sufficient condition for eliminating these oscillations – fixing the rudder (keeping feet on the rudder pedals).

REFERENCES

1. EUROPEAN AVIATION SAFETY AGENCY [EASA]. *Certification specifications for Sailplanes and Powered Sailplanes*: CS-22. 14 November, 2003, no. 2003/13/RM, 141 p.

2. RUGAITIS, A., *et al.* Modeling, experimental research and critical parameter analysis of glider's dynamic characteristics. *Mechanika*, 2010, no. 6(86), p. 38–42.
3. VITTALA, N.G.V.; PANKAJ, A.C.; VENKATASUBRAMANAYAM, D.V. Flutter analysis of a composite light trainer aircraft. *Journal of Scientific and Industrial Research*, 2010, vol. 69, iss. 2, p. 113–120.

LIST OF PUBLICATIONS ON THE TOPIC OF DISSERTATION

In the reviewed scientific periodical journals

1. Andrikaitis, Marius; Fedaravičius, Algimantas. Development of a finite element model of the sailplane fuselage // *Journal of Vibroengineering*. ISSN 1392-8716. 2012, Vol. 14, iss. 3, p. 1390-1398. [ISI Web of Science].
2. Andrikaitis, Marius; Fedaravičius, Algimantas. Modal and flutter analysis of the sailplane LAK-17B using numerical methods // *Transport*. ISSN 1648-4142. 2014, Vol. 29, no. 1, p. 84-89. [ISI Web of Science].

In the proceedings of international conferences

1. Andrikaitis, Marius; Fedaravičius, Algimantas; Paknys, Leopoldas. Finite element modeling of the sailplane landing gear // *Transport Means - 2010: proceedings of the 14th international conference*, Kaunas, October 21-22, 2010. ISSN 1822-296X. 2010, p. 168-170.

In the abstracts of papers of international conferences

1. Sakalauskaitė, Aurelija; Andrikaitis, Marius. Teaching Mathematics Using Theoretical Model // IX nordic – baltic agrometrics conference: abstracts of papers, Kaunas, June 11–13, 2014 / Aleksandras Stulginskis University Kaunas, 2014. p. 23–25.

OTHER PUBLICATIONS

In the proceedings of international conferences

1. Paknys, Leopoldas; Andrikaitis, Marius; Fedaravičius, Algimantas; Analysis of the power required for gyroplane // *Transport Means - 2009: proceedings of the 13th international conference*, Kaunas, October 22-23, 2009. ISSN 1822-296X. 2009, p. 179-181.
2. Paknys, Leopoldas; Andrikaitis, Marius. Gyroplane trim in horizontal flight // *Transport Means - 2012: proceedings of the 16th international conference*, Kaunas, October 25-26, 2012. ISSN 1822-296X. 2012, p. 225-227.

INFORMATION ABOUT THE AUTHOR

Name, Surname: Marius Andrikaitis
Date and place of birth: 20 August 1985, Kaunas, Lithuania
E-mail: marius.andrikaitis@gmail.com

Education

2009-09 – 2013-08 Doctoral student at Kaunas University of Technology in the field of Transport Engineering Sciences
2007-09 – 2009-07 Kaunas University of Technology, Master of Sciences in Transport Engineering
2003-09 – 2007-07 Kaunas University of Technology, Bachelor of Sciences in Transport Engineering
1992-09 – 2003-06 Kaunas district "Noreikiškės" secondary school.

Working practice

since 2007-08 till present Design engineer in JSC "Sportinė aviacija ir Ko"
since 2013-07 till present Assistant in Kaunas University of Technology, Department of Transport Engineering.

REZIUMĖ

Disertacijos struktūra ir apimtis

Disertaciją sudaro įvadas, penki skyriai, išvados, literatūros sąrašas ir autoriaus publikacijų sąrašas.

Disertacijos apimtis – 109 puslapiai. Darbe yra 102 numeruotos formulės, pateikta 115 paveikslų ir 24 lentelės. Rašant disertaciją naudotasi 82 literatūros šaltiniais.

Pirmame skyriuje analizuojama: (a) sportinių sklandytuvų skirstymas į klases ir kiekvienai klasei būdingos geometrinės ir skrydžio charakteristikos, (b) sklandytuvų kritiniai režimai ir jų apkrovų normavimas pagal CS-22, (c) šiuo metu naudojami aviacinių konstrukcijų kritinių režimų tyrimo metodai.

Antrame skyriuje detalizuojama sklandytuvo LAK-17B modeliavimo ir jo kritinių režimų tyrimo eiga. Apžvelgiami tyrimo metodai, realizuoti darbui atlikti naudojtoje programinėje įrangoje: (a) sluoksniuotų medžiagų modeliavimas ir jų stiprumo įvertinimo kriterijai, (b) tikrinių reikšmių apskaičiavimas ir flaterio analizė.

Trečiame skyriuje aprašyta sklandytuvo skaitinių modelių kūrimo metodika. Analizuojami modeliuojamo objekto (sklandytuvo LAK-17B) pagrindinių konstrukcijos elementų – fiuzeliažo, sparnų, uodegos plokštumų, važiuoklės – konstrukciniai ypatumai, išskiriami ir detalizuojami kiekvieno konstrukcinio elemento modelių kūrimo etapai.

Ketvirtame skyriuje aprašytas sukurtų modelių parametrų nustatymas. Šiame darbe modelio parametrų rinkiniu vadinamas apkrovų rinkinys, apkrovų pridėties taškų koordinatės ir optimalių baigtinių elementų tinklo tankumą apibūdinantys dydžiai.

Penktame skyriuje pateikti sklandytuvo LAK-17B kritinių režimų tyrimo naudojant sukurtus modelius rezultatai. Skaitiniu modeliavimu gauti duomenys: (a) didžiausios sklandytuvo važiuoklę veikiančios apkrovos ir važiuoklės konstrukcijos atsargos koeficientai, (b) fiuzeliažo ir uodegos plokštumų atsargos koeficientai, (c) kritiniai sklandytuvo galinės dalies flaterio greičiai.

Darbo pabaigoje pateiktos disertacinio darbo išvados, kurios atspindi pagrindinius atliktų tyrimų rezultatus.

Darbo tikslas

Sertifikuojamo sklandytuvo LAK-17B skaitinių modelių sukūrimas ir šios konstrukcijos antžeminių ir skrydžio kritinių režimų ištyrimas įvertinant konstrukcijos sertifikavimo reikalavimų atitikimą.

Uždaviniai

1. Sukurti sklandytuvo LAK-17B važiuoklės, fiuzeliažo ir aerodinaminių plokštumų skaitinius modelius ir pagrįsti modelių tinkamumą pasirinktiems kritiniams režimams tirti.

2. Naudojant modelius, ištirti važiuklės kritinius režimus nustatant konstrukciją veikiančias antžemines apkrovas ir konstrukcijos stiprumo bei standumo parametrus.
3. Naudojant modelius, ištirti fiuzeliažo ir uodegos plokštumų kritinius režimus nustatant konstrukciją veikiančias skrydžio apkrovas ir konstrukcijos stiprumo parametrus.
4. Atlikti sklandytuvo galinės dalies flaterio analizę nustatant galinės dalies svyravimų susidarymo sąlygas.

Mokslinis naujumas

1. Sukurtas modelių rinkinys, kurį naudojant ištirta atskirų sklandytuvo LAK-17B konstrukcinių elementų parametrų kitimo įtaka bendram konstrukcijos darbui.
2. Nustatyta, kad tiriamas sklandytuvas atitinka skraidymo aparatams keliamus sertifikavimo reikalavimus.

Darbo praktinė vertė

1. Sudaryta nauja sklandytuvo LAK-17B ir jo modifikacijų konstrukcinių elementų skaitinių modelių kūrimo naudojant šiuolaikinius įrankius metodika.
2. Metodika pritaikyta sklandytuvo skaitiniams modeliams kurti.
3. Sukurti modeliai panaudoti sklandytuvo LAK-17B kritiniams režimams tirti.
4. Tyrimo rezultatai pritaikyti praktiškai, sertifikuojant sklandytuvą.

Ginamieji teiginiai

1. Tyrimui naudojami sklandytuvo LAK-17B skaitiniai modeliai įvertina (a) konstrukcijos geometrinius ypatumus, (b) konstrukcijos elementų šarnyrinius sujungimus, (c) kompozitų sluoksnių charakteristikas, (d) konstrukcijos masių pasiskirstymą.
2. Sklandytuvo LAK-17B važiuklės konstrukcijos stiprumas ir standumas atitinka sklandytuvams ir motorizuotiems sklandytuvams keliamus sertifikavimo reikalavimus CS-22.
3. Sklandytuvo LAK-17B fiuzeliažo ir uodegos plokštumų konstrukcijos stiprumas atitinka skrydžio apkrovų atvejams keliamus sertifikavimo reikalavimus CS-22. Avarinių režimų atveju fiuzeliažo priekinės dalies konstrukcija turėtų būti modifikuota (sustiprinta).
4. Sklandytuvo LAK-17B skrydžio greičių intervale 90...150 km/h susidarančius konstrukcijos svyravimus sukelia laisvo posūkio vairo svyravimas. Nekeičiant posūkio vairo valdymo sistemos konstrukcijos, būtina ir pakankama sąlyga šiems svyravimams užgesinti – posūkio vairo valdymo pedalų fiksavimas (prispaudimas kojomis).

IŠVADOS

1. Sukurti sklandytuvo skaitiniai modeliai, įvertinantys (a) konstrukcijos geometrinius ypatumus, (b) konstrukcijos elementų šarnyrines jungtis, (c) kompozitų sluoksnių charakteristikas, (d) konstrukcijos masių pasiskirstymą. Remiantis modeliavimo ir bandymo rezultatais, (a) modeliavimu ir bandymu nustatytų konstrukcijos įlinkių skirtumas neviršija 10%, (b) modeliavimu nustatytos konstrukcijos stabilumo praradimo zonos ir stabilumo atsargos koeficientai atitinka bandymu nustatytas vertes, (c) modeliavimu ir bandymu nustatytų sklandytuvo laisvųjų svyravimų formų ir svyravimų dažnių kitimo pobūdis vienodas, todėl modelio tikslumas pasirinktiems kritiniams režimams tirti yra pakankamas.
2. Sklandytuvo LAK-17B pagrindinės važiuoklės stiprumo atsargos koeficientas didesnis už 1,5; važiuoklės konstrukcijos elementų įlinkiai tupdymo metu nėra ribiniai, o tupdymo perkrovos koeficientas yra lygus 4 ir neviršija leistinos 4,5 ribos, todėl sklandytuvo LAK-17B važiuoklės stiprumas ir standumas atitinka sertifikavimo reikalavimus CS-22.
3. Sklandytuvo LAK-17B fiuzeliažo ir uodegos plokštumų stiprumo atsargos koeficientai didesni už 1,5, o fiuzeliažo stabilumo atsargos koeficientas yra lygus 1,5. Sklandytuvo fiuzeliažo ir uodegos plokštumų stiprumas ir standumas didžiausių skrydžio apkrovų atvejais atitinka sertifikavimo reikalavimus CS-22. Avarinių režimų apkrovų atveju fiuzeliažo priekinės dalies stiprumo ir stabilumo atsargos koeficientai yra mažesni už 1,5, todėl būtinas konstrukcijos sustiprinimas.
4. Remiantis sudarytomis sklandytuvo LAK-17B slopinimo ir svyravimų dažnių priklausomybėmis nuo skridimo greičio, skrydžio greičių intervale 90...150 km/h susidarančius konstrukcijos galinės dalies svyravimus sukelia laisvo nesubalansuoto posūkio vairo svyravimas. Nekeičiant posūkio vairo valdymo sistemos konstrukcijos, būtina ir pakankama sąlyga šiems svyravimams užgesinti – posūkio vairo valdymo pedalų fiksavimas (prispaudimas kojomis).

UDK 629.743.33.02(043.3)

SL344. 2014-11-05, 1,75 leidyb. apsk. I. Tiražas 70 egz. Užsakymas 604.

Išleido leidykla „Technologija“, studentų g. 54, 51424 Kaunas

Spausdino leidyklos „Technologija“ spaustuvė, Studentų g. 54, 51424 Kaunas